ACS APPLIED MATERIALS & INTERFACES

Letter

www.acsami.org

Waterproof Active Paper via Laser Surface Micropatterning of Magnetic Nanoparticles

G. Chitnis[†,‡] and B. Ziaie*[,‡,§]

[†]School of Mechanical Engineering, [§]School of Electrical and Computer Engineering, [‡]Birck Nanotechnology Center, Purdue University, West Lafayette, Indiana, United States

ABSTRACT: Paper is one of the oldest and most abundant materials known to man. Recently, there has been a considerable interest in creating paper devices by combining paper with other functional materials. In this letter, we demonstrate a simple fabrication technique to create water-resistant ferro-patterns on wax paper using CO_2 laser ablation. A resolution of about 100 μm is achieved which is mostly limited by the cellulose fiber size (~50 μm) in the wax paper and can be improved by using a smaller cellulose matrix. Laser ablation results in modification of surface morphology and chemistry, leading to a change in surface energy. We also present a 2D model for ferrofluid deposition relating the size of the pattern to the amount of ferroparticles deposited on the surface. Finally, a paper gripper is presented to demonstrate advantages of our technique, which allows microscale patterning and machining in a single step.

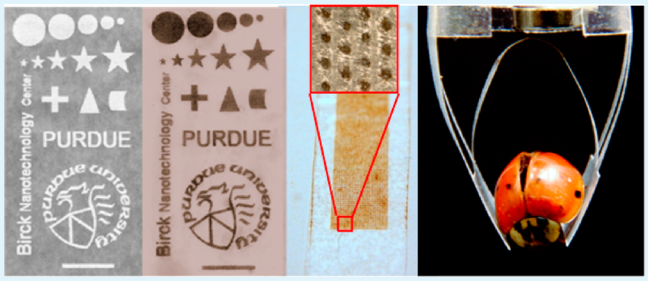

KEYWORDS: *laser ablation, magnetic, actuators, patterning, ferrofluid*

1. INTRODUCTION

Paper is one of the oldest and most abundant materials known to man. The technology of paper-making has been evolved over thousands of years. As a result, production of various kinds of papers has now become extremely economical. Paper is not only cheap and easy to manufacture but it is also almost 100% cellulose, a biodegradable and annually renewable resource. Apart from its basic utility as a writing medium, paper has also been employed in other applications such as packaging, filtering, and art/craft. Recently, there has been a considerable interest in paper as a low cost substrate to create microfluidic devices,[1−8] sensors,[9,10] electronics,[11−16] and actuators.[17,18]

In this work, we present a novel method to pattern magnetic material onto commercially available wax paper which subsequently can be used to create magnetic microstructures for tagging, sensing, and actuating applications. We previously reported on a method to create paper-based magnetic actuators by completely soaking a hydrophilic paper in ferrofluid and laser-machining the magnetic substrate to the desired shape.[19] More recently, Fragouli et al[20] reported on superparamagnetic cellulose fibers through chemical reaction functionalization. In both these methods, nanoparticles are present uniformly throughout the paper matrix; preventing a fine spatial control. The process described in this paper enables the creation of microscale (~100 μm) wax-embedded magnetic patterns on paper only in selected areas. In addition, this technique allows simultaneous machining of the substrate by cutting through the paper.

2. EXPERIMENTAL SECTION

2.1. Laser Ablation. The patterning technique relies on laser ablation of hydrophobic surface of wax paper to create hydrophilic areas which are later selectively coated with aqueous ferrofluid, as shown in Figure 1a−d. A computer-controlled CO_2 laser cutting and engraving system [Universal Laser System, Inc. Professional Series, maximum power 60 W, maximum speed 2 mm/ms, wavelength 10 μm, Continuous Wave (CW) mode] is used to directly write CAD-generated patterns onto a wax paper. To avoid completely cutting through the paper (instead of selective surface modification), the laser power and scanning speed has to be carefully selected. Higher laser power and lower scanning speed results in complete removal of surface and bulk material (i.e., paper), creating through-paper defects. For the wax paper selected in our experiments (Raynolds Cut-Rite Wax Paper, ~30 μm-thick), the laser source is controlled at 15% of its maximum power and is operated at a maximum scanning speed (2 mm/ms). Laser interaction with the wax layer modifies the surface and creates hydrophilic patterns, Figure 1a. The paper can also be machined to desired shape in the same step by increasing the power to 50% of its maximum. As a result, one can achieve precise machining and patterning without any alignment step, which cannot be accomplished by other paper patterning techniques such as lithographic patterning[1] and wax printing.[21]

Received: June 19, 2012
Accepted: August 31, 2012
Published: August 31, 2012

   dx.doi.org/10.1021/am3011065 | ACS Appl. Mater. Interfaces 2012, 4, 4435−4439

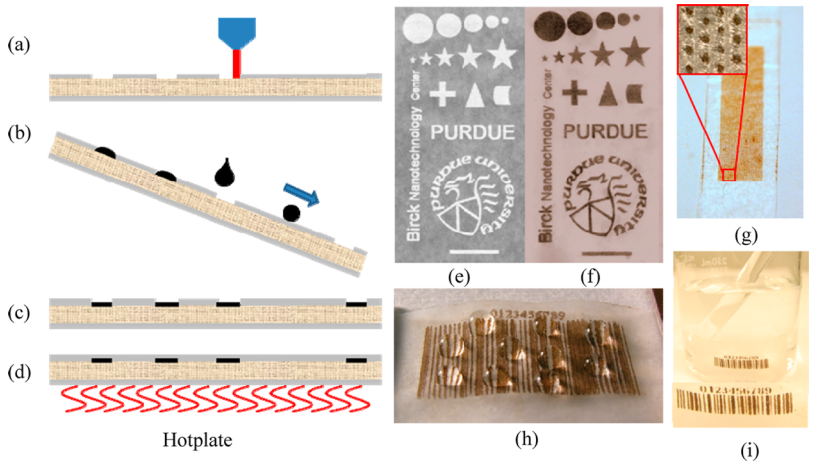

Figure 1. (a–d) Process of patterning ferrofluid on wax paper using laser ablation, (e) wax paper after laser ablation (scale bar = 15 mm), (f) wax paper after ferrofluid deposition (scale bar = 15 mm), (g) array of dots (diameter,: 100 μm; pitch, 300 μm) patterned on wax paper, (h) barcode pattern after heat treatment, (i) barcode pattern immersed in water after heat treatment.

2.2. Ferromagnetic Nanoparticle Coating. The ablated and machined samples are coated with aqueous ferrofluid (EMG-605, particle size 10 nm, Ferrotec Corp.), Figure 1b, and dried out at room temperature, Figure 1c. The ferrofluid is retained in laser-ablated hydrophilic areas and rolls away in unablated hydrophobic ones, forming desired patterns of ferromagnetic nanoparticles. Finally, the patterned paper is heat treated in order to melt the wax, covering the dried ferrofluid, Figure 1d.

2.3. Characterization. To understand the changes in physical microstructure of the surface following laser ablation, we observed wax paper under scanning electron microscope (field-emission SEM, Hitachi S-4800) with an acceleration voltage of 10 kV. High resolution images are obtained to study the microstructure of paper after laser ablation and coating with nanoparticles. Further, X-ray photospectrometric (XPS) analysis is performed to analyze the change in chemical composition of the surface. Contact angle is measured using a gonimeter to quantify the change in surface energy.

3. RESULTS AND DISCUSSION

3.1. Laser Ablation. Figure 1e shows various magnetic patterns on wax paper having a large variety of geometries and dimensions. The contact angle of water on wax paper is 108°, which is reduced to 70° when treated with laser. The treated area does tend to absorb a small amount of water which does not penetrate deep or move laterally since only surfaces of cellulose fibers are exposed. White regions in Figure 1e are the ablated areas which subsequently turned brown after exposure to ferrofluid, Figure 1-f. Figure 1g shows an array of circles with 100 μm diameter and 300 μm pitch. Panels h and i in Figure 1 show the wax coated samples after heat treatment. Water droplets bead up, even on the patterned areas, Figure 1h, demonstrating a complete wax coating. Even with an overnight water immersion, no significant loss of magnetic nanoparticles is observed, Figure 1i.

Figure 2 shows the SEM images at various magnifications. As can be seen, there is a noticeable difference in the surface roughness following laser ablation accompanied by the presence of porous microstructure which are absent in unablated regions, Figure 2b, c. Nonablated wax paper area shown in Figure 2c clearly illustrates the presence of cellulose

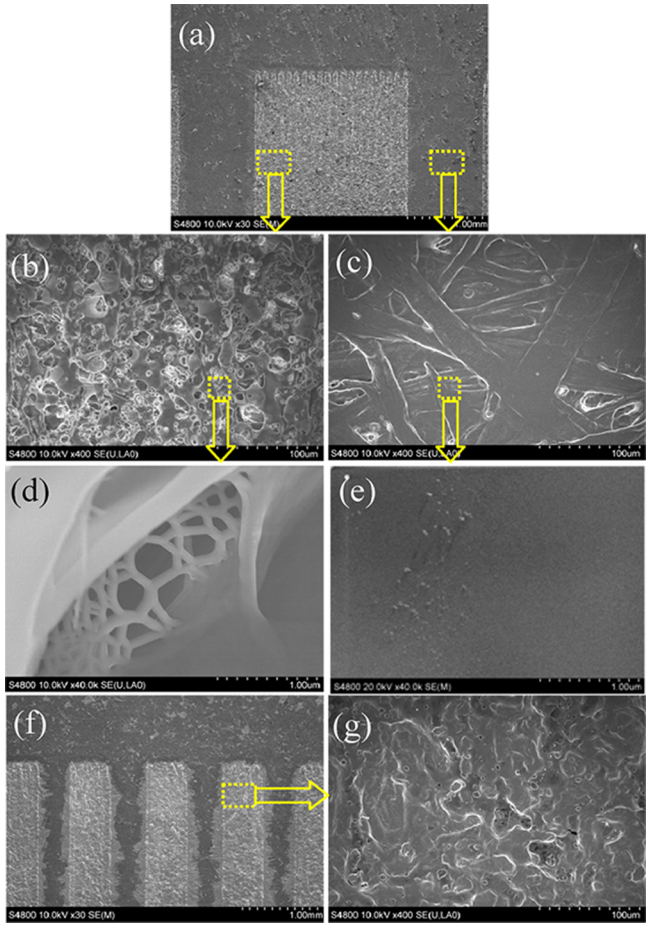

Figure 2. (a) SEM image of wax paper with ablated stripe (×30), (b) a higher-resolution image (×400) of ablated area, (c) wax paper surface (×400), (d) laser ablated surface showing nanofibers (×40 000), (e) wax paper surface (×40 000), (f) (×30) wax paper after ferrofluid deposition, and (g) a higher-resolution image of laser ablated surface after ferrofluid deposition (×400).

fibers larger than 10 μm. High-resolution image of the laser treated area, Figure 2d, shows the presence of nanofiber-net, which are not observed before laser treatment or after reheating of the samples. We hypothesize that these nanofibers are

dx.doi.org/10.1021/am3011065 | ACS Appl. Mater. Interfaces 2012, 4, 4435–4439

formed due to melting and resolidification of wax, with cellulose fibers providing anchor points for these wax nanofibers. Figure 2e shows a high-resolution SEM image of an untreated wax paper lacking the nanofiber nets. Images f and g in Figure 2 are images of a ferroparticle-deposited surface at low and high magnifications. Although the surface is still very rough, most of the micropores seem to be filled with ferroparticles.

Along with nanofiber formation, thermal interaction of laser with wax and atmospheric oxygen leads to oxidation of surface, resulting in exposed C−OH, −COOH groups which are polar and hence hydrophilic in nature. Figure 3 shows the wide and

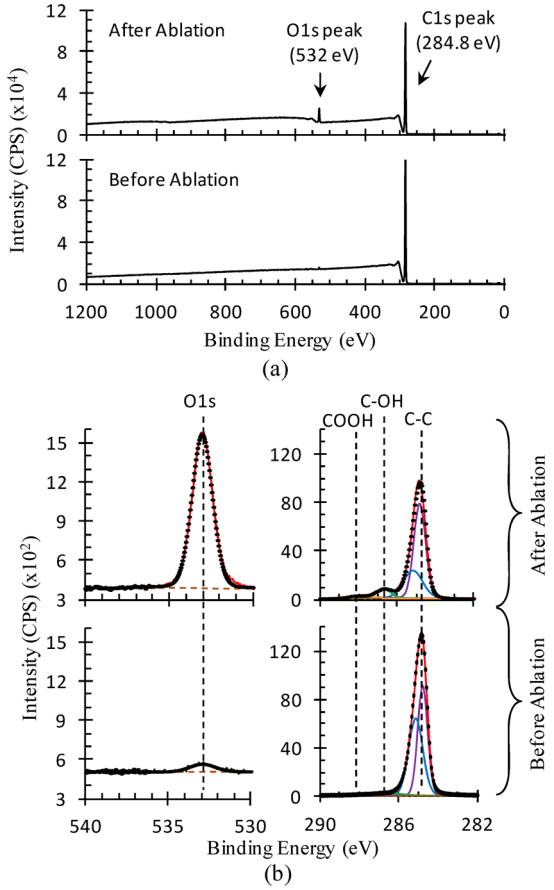

Figure 3. (a) Wide XPS spectra showing presence of oxygen in laser ablated region, (b) high-resolution XPS spectra at O1s and C1s peaks showing presence of −C−OH and −COOH bonds in laser ablated region.

high-resolution XPS spectra, before and after laser ablation. A strong peak for oxygen (O1s peak) is detected in the case of laser ablated surface but no such peak is observed for original wax paper (Figure 3a). High-resolution XPS spectra, Figure 3-b, shows weak presence of oxygen in the wax paper but intensity is significantly enhanced after laser ablation. Also, carbon peak shows significant increase in intensity corresponding to −COH and −COOH groups, accompanied by reduction in intensity of C−C peak. This shows that laser ablation aided breaking C−C bonds and oxidizing the carbon to form −COOH and C−OH bonds. Overall, although exposed cellulose fibers can contribute to hydrophilicity of the ablated areas, change in chemical structure also plays an important role. Exposed areas of cellulose fiber have the tendency to absorb some water but this is limited because the rest of the fibers are still soaked in solid wax. When a droplet of water is placed on laser treated surface, it does not soak inside or seep laterally unlike other water absorbing papers.

3.2. Nanoparticle Patterning. For most practical applications, it is important to know the amount of nanoparticles deposited on the surface. We developed an analytical equation to estimate the mass of ferroparticles retained by hydrophilic patterns. Figure 4a shows the schematic of ferrofluid retained on laser ablated porous area. As expected, some fluid penetrates the fibrous network and voids created due to ablation while the rest stays on the surface forming a specific contact angle. It is difficult to estimate the depth of penetration of nanoparticles; however, because only the surface is treated with laser and rest of the paper stays soaked in solid wax, we do not expect ferrofluid to penetrate to the other side which is confirmed by the fact that backside does not show the presence of ferroparticles.

Assuming that the meniscus of ferrofluid on straight lines takes the shape of a cylindrical surface, total volume of ferrofluid in one continuous hydrophilic strip can be given by

$$V = V_0 + \left(\theta R^2 - \frac{w(R-h)}{2}\right)L \tag{1}$$

where V is the total volume of ferrofluid, V_0 is the volume absorbed in the laser-created voids, θ is the contact angle, R is the meniscus radius of curvature, w is the width of laser ablated area, h is the height of liquid from surface of paper, and L is the length of the pattern. Volume absorbed in the fibrous mesh, V_0, should be proportional to the depth of fibrous network, or

$$V_0 = kLwt \tag{2}$$

where t is the depth of laser-created fibrous network and k (<1) is a proportionality constant.

Substituting V_0, $R = w/2\sin\theta$, $R - h = w/2\tan\theta$ in eq 1, and multiplying by weight concentration C, we get the total mass (M) of ferroparticles deposited on a dry sample

$$M = CNwL\left[kt + w\left(\frac{\theta}{4\sin^2\theta} - \frac{1}{4\tan\theta}\right)\right] \tag{3}$$

$$\text{mass per unit area} = \frac{M}{A} = \frac{M}{NwL} = C\left[kt + w\left(\frac{\theta}{4\sin^2\theta} - \frac{1}{4\tan\theta}\right)\right] \tag{4}$$

where N is number of ablated strips with dimensions of Lw. Equation 4 clearly suggests that the amount ferrofluid deposited per unit area depends not only on the concentration of the ferrofluid but also on the width of patterns (w) and contact angle (θ). To verify this analytical expression, we created samples with NwL = 30 mm^2 (L = 5 mm, N = 1−10), Figure 4b. Samples were weighed before and after deposition and the difference was recorded as the added mass of ferroparticles (M). Figure 4d shows the concentration of added mass (M/A) plotted against width (w) showing that the mass concentration of ferrofluid deposited on the patterned area increases with increasing the width of pattern as suggested by eq 4. The line in the plot shows mass concentration calculated using eq 4. Although the rise is linear for small widths, it starts to saturate and deviates from the calculated value for wider patterns. This discrepancy arises because of the assumption of droplet shape

dx.doi.org/10.1021/am3011065 | ACS Appl. Mater. Interfaces 2012, 4, 4435−4439

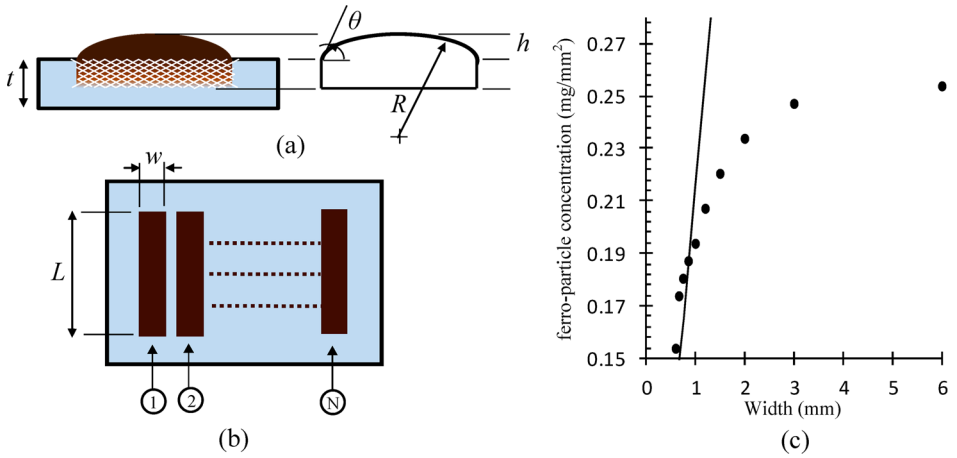

Figure 4. (a) Schematic showing geometric parameters of ferrofluid retained on porous hydrophilic laser ablated surface, (b) sample used to characterize ferrofluid deposition as a function of geometry, and plot showing relationship between mass of deposited ferroparticles and pattern width (w).

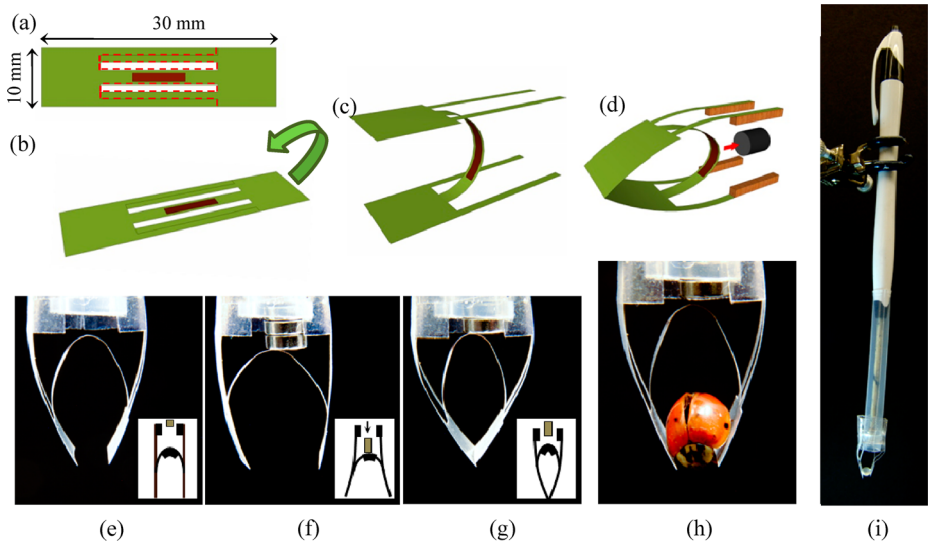

Figure 5. A magnetic gripper fabricated using the laser surface treatment and micromachining method. Wax paper cut at dotted red line and ablated in brown area (a), ferrofluid is deposited in the ablated area and paper is folded (b), gripper in folded position (c), anchored gripper in presence of a permanent magnet (d), gripper in "natural open position" (e), in "forced open position" (f), in "closed position" (g), gripper holding a ladybug (h), and the complete assembly of gripper with clicker pen (i).

on the surface (deposited fluid volume is approximated as horizontal cylindrical segment), which fails for large volumes of fluid because of gravitational force. The expression used for volume, which assumes a uniform cross-section, does not hold true for wider samples as width becomes comparable to the length. Overall, per unit area concentration of the ferroparticle deposit is proportional to the pattern size until the point of saturation.

3.3. Application as an Actuator. The patterning and machining method described here can be used for various applications such as magnetic tagging, sensors, and actuators. For demonstration, we designed and fabricated a paper based gripper that can hold objects by utilizing attractive force of small permanent magnets (R311, K&J Magnetics Inc.). Figure 5 shows the schematic and the actual fabricated device. As shown in Figure 5a, wax paper was cut along dotted lines and ablated in the brown regions. The cantilevers were cut and patterned in the same step by only altering the laser power level. Subsequently, ferrofluid was deposited in the ablated area and the structure was folded as shown in Figure 5b to bring holding pads to face each other (Figure 5c) and four anchor points of the actuator glued to a fixed anchor point (Figure 5d). To ease the process of moving permanent magnet back and forth, gripper was mounted on the tip of a clicker pen whose refill was replaced by a thin rod with the magnet at the tip. The distance was adjusted such that one click opens the holding pads whereas a subsequent one closes it. Figure 5e–g show the gripper in various positions (insets show simple sketches depicting the actuation mechanism/sequence). In its "natural open position" two arms of gripper stay apart, Figure 5d. When the magnet is brought closer to the ferrofluid patterned area, it initially pushes the assembly mechanically to open up the holding ends even more (Figure 5f) to its "forced open position". After completing the first click (corresponding to protruding position while writing), holding pads remain in a "closed position" due to the attractive magnetic force, Figure 5g. During this phase, the gripper can be used to hold objects. When pen is clicked for a second time, the magnet first pushes

on the assembly to open up the holding pads releasing the grabbed object and then settles in its "natural open position". It is important to note that in the "forced open position", the gripper has a larger jaw size allowing it to hold bigger objects. Use of magnetic force instead of adhesive for this mechanical movement facilitates easy replacement of paper-gripper thus avoiding contamination. Also, an electromagnet can be used to activate gripper using an electric switch instead of mechanical movement but that demands a currents source which makes it unnecessarily complicated. Figure 5h shows a ladybug held using the paper gripper. Figure 5i shows the whole assembly of the actuator including the clicker pen. With this specific configuration (actuator size (30 mm long and 10 mm wide), clicker stroke length (6 mm) and ferro-particle concentration ($0.7\ mg/mm^2$)) the gripper could hold samples weighing up to 50 mg.

4. CONCLUSIONS

We successfully demonstrated a simple fabrication technique to create water-resistant ferro-patterns on the wax paper using CO_2 laser ablation. A resolution of about 100 μm was achieved which is mostly limited by the cellulose fiber size (~50 μm) in the wax paper and can be improved by using a smaller cellulose matrix. Laser ablation resulted in modification of surface morphology and chemistry leading to a change in surface energy. We also presented a 2D model for ferrofluid deposition relating the size of the pattern to the amount of ferroparticles deposited on the surface. Our model correctly predicted that larger patterns lead to higher mass concentration until the point of saturation. Finally, we designed a paper gripper based on magnetic actuation to demonstrate advantages of our technique which allows microscale patterning and machining in a single step.

AUTHOR INFORMATION

Corresponding Author

*Address: 1205 West State Street, West Lafayette, Indiana 47907. E-mail: bziaie@purdue.edu.

Notes

The authors declare no competing financial interest.

ACKNOWLEDGMENTS

This work was supported by the National Science Foundation (Grant ECCS-1128169). The authors thank Dr. Dmitry Zemlyanov for his help with XPS analysis.

REFERENCES

(1) Martinez, A. W.; Phillips, S. T.; Butte, M. J.; Whitesides, G. M. *Angew. Chem., Int. Ed.* **2007**, *46*, 1318−1320.
(2) Martinez, A. W.; Phillips, S. T.; Carrilho, E.; Thomas, S. W.; Sindi, H.; Whitesides, G. M. *Anal. Chem.* **2008**, *80*, 3699−3707.
(3) Martinez, A. W.; Phillips, S. T.; Wiley, B. J.; Gupta, M.; Whitesides, G. M. *Lab Chip* **2008**, *8*, 2146−2150.
(4) Bruzewicz, D. A.; Reches, M.; Whitesides, G. M. *Anal. Chem.* **2008**, *80*, 3387−3392.
(5) Martinez, A. W.; Phillips, S. T.; Nie, Z.; Cheng, C.-M.; Carrilho, E.; Wiley, B. J.; Whitesides, G. M. *Lab Chip* **2010**, *10*, 2499−2504.
(6) Klasner, S. a; Price, A. K.; Hoeman, K. W.; Wilson, R. S.; Bell, K. J.; Culbertson, C. T. *Anal. Bioanal. Chem.* **2010**, *397*, 1821−1829.
(7) Li, X.; Tian, J.; Garnier, G.; Shen, W. *Colloids Surf., B* **2010**, *76*, 564−570.
(8) Chitnis, G.; Ding, Z.; Chang, C.-L.; Savran, C. a; Ziaie, B. *Lab Chip* **2011**, *11*, 1161−1165.
(9) Liu, X.; Mwangi, M.; Li, X.; O'Brien, M.; Whitesides, G. M. *Lab Chip.* **2011**, *11*, 2189−2196.
(10) Tao, H.; Chieffo, L. R.; Brenckle, M. a; Siebert, S. M.; Liu, M.; Strikwerda, A. C.; Fan, K.; Kaplan, D. L.; Zhang, X.; Averitt, R. D.; Omenetto, F. G. *Adv. Mater.* **2011**, *23*, 3197−3201.
(11) Eder, F.; Klauk, H.; Halik, M.; Zschieschang, U.; Schmid, G.; Dehm, C. *Appl. Phys. Lett.* **2004**, *84*, 2673−2675.
(12) Lamprecht, B.; Thünauer, R.; Ostermann, M.; Jakopic, G.; Leising, G. *Phys. Status Solidi (a)* **2005**, *202*, R50−R52.
(13) Hu, L.; Choi, J. W.; Yang, Y.; Jeong, S.; Mantia, F.; La; Cui, L.-F.; Cui, Y. *Proc. Natl. Acad. Sci. U.S.A.* **2009**, *106*, 21490−4.
(14) Siegel, A. C.; Phillips, S. T.; Dickey, M. D.; Lu, N.; Suo, Z.; Whitesides, G. M. *Adv. Funct. Mater.* **2010**, *20*, 28−35.
(15) Jabbour, L.; Gerbaldi, C.; Chaussy, D.; Zeno, E.; Bodoardo, S.; Beneventi, D. *J. Mater. Chem.* **2010**, *20*, 7344−7347.
(16) Tobjörk, D.; Österbacka, R. *Adv. Mater.* **2011**, *23*, 1935−61.
(17) Kim, J.; Seo, Y. B. *Smart Mater. Struct.* **2002**, *11*, 355−360.
(18) Zhou, J.; Fukawa, T.; Shirai, H.; Kimura, M. *Macromol. Mater. Eng.* **2010**, *295*, 671−675.
(19) Ding, Z.; Wei, P.; Chitnis, G.; Ziaie, B. *J. Microelectromech. Syst.* **2011**, *20*, 59−64.
(20) Fragouli, D.; Bayer, I. S.; Corato, R.; Di; Brescia, R.; Bertoni, G.; Innocenti, C.; Gatteschi, D.; Pellegrino, T.; Cingolani, R.; Athanassiou, A. *J. Mater. Chem.*. **2012**, *22*, 1662.
(21) Carrilho, E.; Martinez, A. W.; Whitesides, G. M. *Anal. Chem.* **2009**, *81*, 7091−5.

NOTE ADDED AFTER ASAP PUBLICATION

This paper was published on the Web on September 6, 2012. An Acknowledgment paragraph was added afterwards, and the corrected version was reposted on September 11, 2012.